

Supporting Information

Zero-dimensional methylammonium iodo bismuthate solar cells and synergistic interactions with silicon nanocrystals

By Calum McDonald¹, Chengsheng Ni², Vladimir Svrcek³, Mickael Lozac'h³, Paul Connor², Paul Maguire¹, John Irvine² and Davide Mariotti¹

1 Nanotechnology and Integrated Bioengineering Centre, Ulster University, BT37 0QB, UK

2 School of Chemistry, University of St Andrews, KY16 9ST, UK

3 Research Center for Photovoltaics, National Institute of Advanced Industrial Science and Technology (AIST), Tsukuba 305-8568, Japan

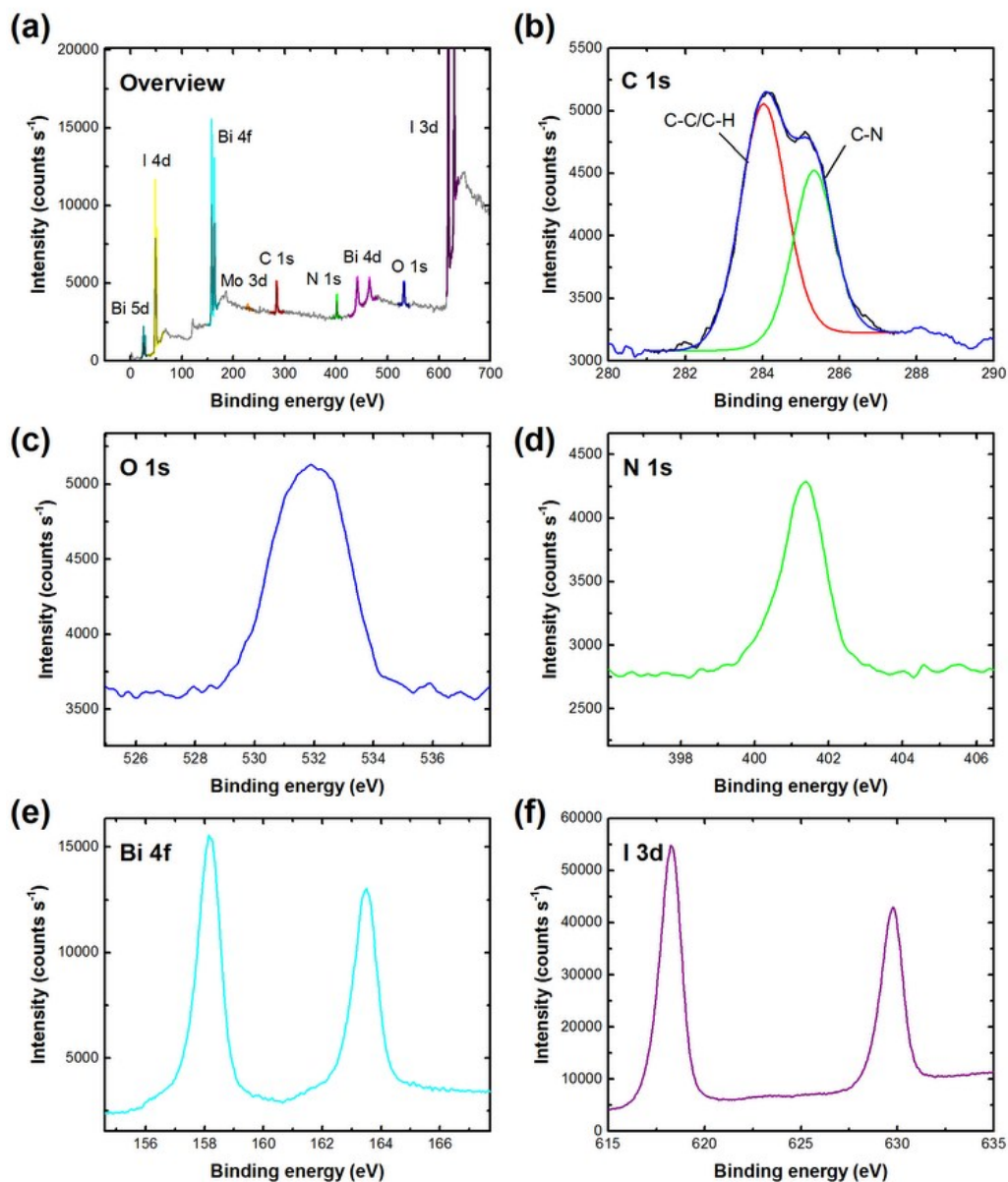


Fig. S1. X-ray photoelectron spectra for MABI thin films spin coated on molybdenum foil. (a) Overview spectrum with the individual spectra superimposed, and (b)-(f) individual spectra for C 1s (b), O 1s (c), N 1s (d), Bi 4f (e), and I 3d (f). All spectra were acquired at room temperature and referenced to the Mo 3d_{5/2} at 228 eV. The splitting of the C 1s peak observed in (b) was previously reported for MAPbI₃.¹ The deconvoluted C 1s peak at 286.5 eV is attributed to carbon bonded to nitrogen (C-N) and the peak at 284 eV is due to carbon bonded to other carbon or hydrogen (C-C, C-H). The O 1s peak at 532 eV corresponds to adsorbed surface species. Hoyer *et al.* observed a Bi-O peak at 530.4 eV in MABI films which could be removed by ion etching,² indicating that it is a surface layer. Also, they observed that the surface O-Bi peak became more pronounced after 1 month of air exposure.² In the results shown here, the samples were prepared and then measured by XPS the following day, and (c) indicates that the surface oxide layer had not yet formed due to

the absence of the Bi-O peak at 530.4 eV. The data shown in this figure is previously published elsewhere.³

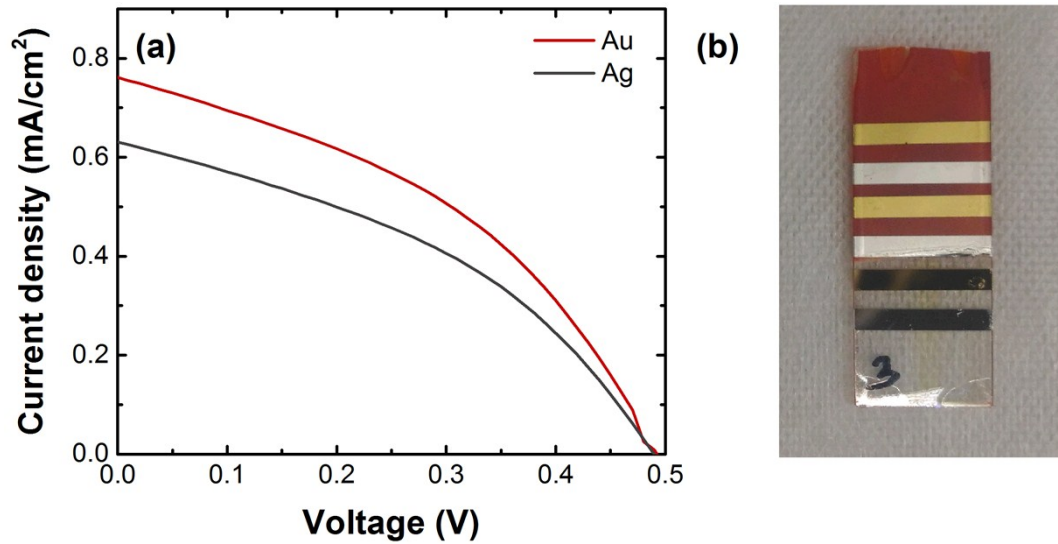


Fig. S2. (a) Current density-voltage (J-V) characteristic for MABI devices produced with Au (red line) and Ag (grey line) contacts. The scan rate for the J-V measurement was 150 mV/s. (b) The corresponding solar cell device, with Ag and Au contacts deposited on the same device to compare the performance of the solar cells in terms of the type of metal contacts directly.

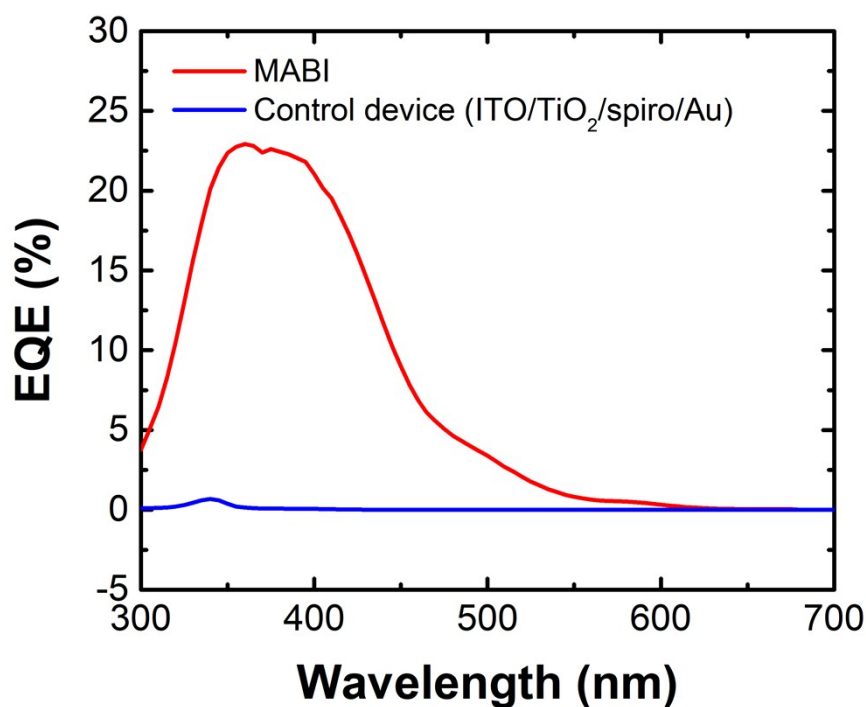


Fig. S3. External quantum efficiency for the champion MABI solar cell (red) with Au contacts and the reference cell without MABI (blue) to highlight that there is no contribution from the transport layers. The structure of the reference cell is ITO/compact-TiO₂/mesoporous-TiO₂/spiro-MeOTAD/Au.

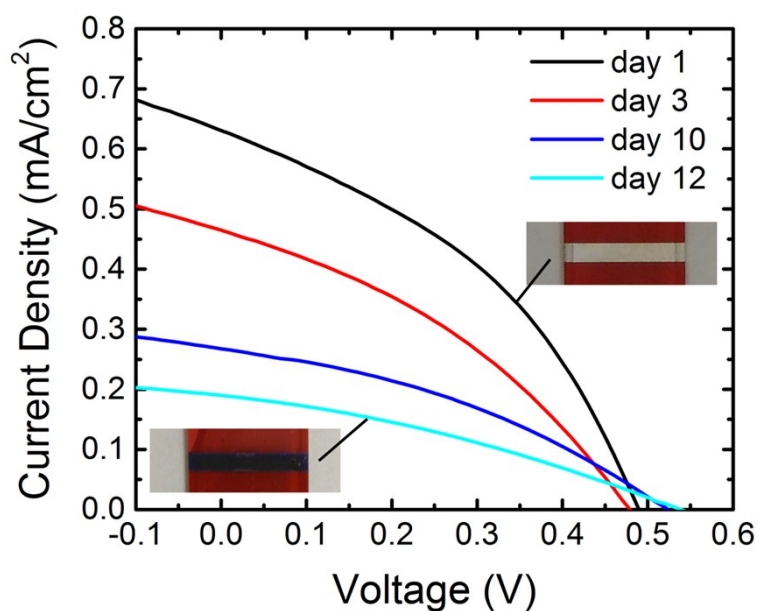


Fig. S4. (a) MABI solar cell aging with Ag contacts over a 12-day period when stored in ambient conditions, with photographs of the corresponding Ag metal contacts as-prepared and after 12 days.

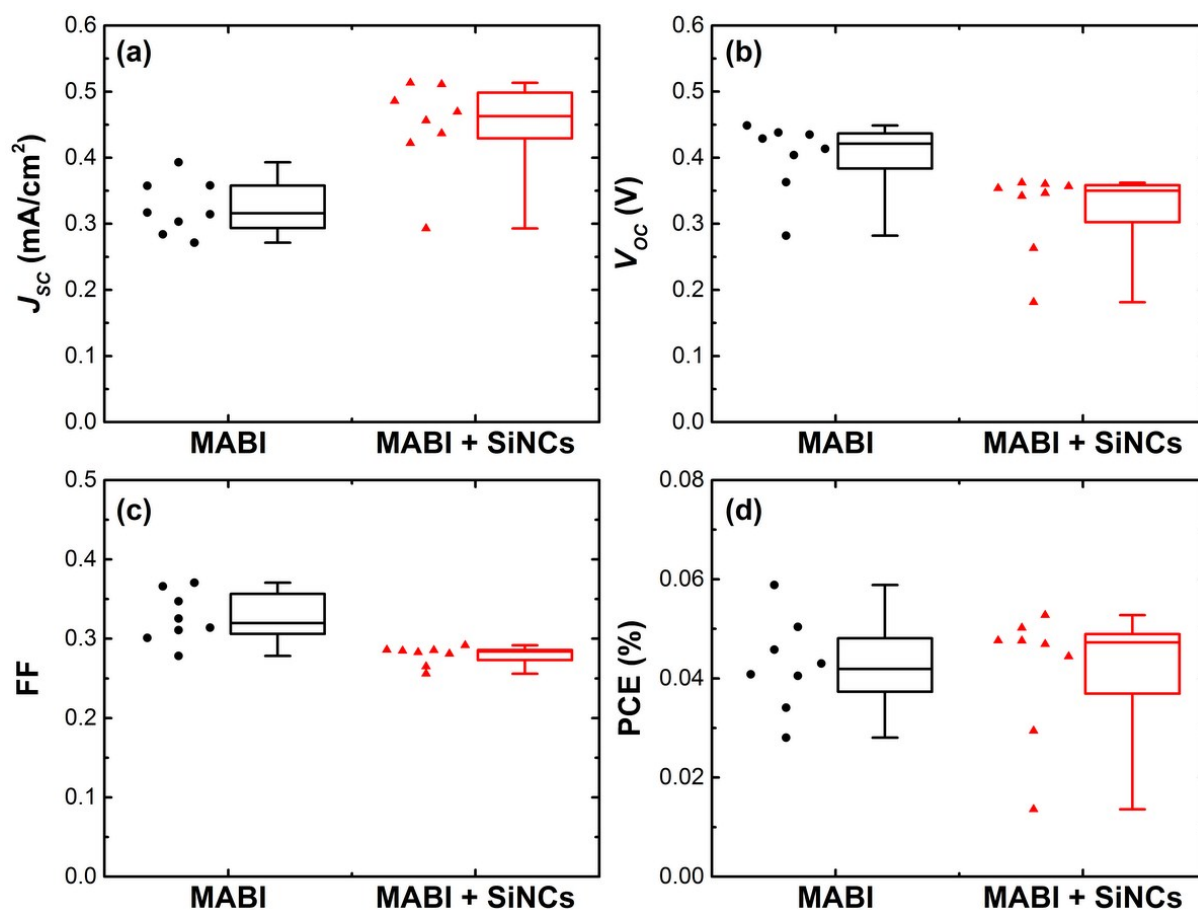


Fig. S5. Performance statistics for devices produced on the same day for 8 MABI devices (black circles) and 8 MABI devices with incorporated silicon nanocrystals (red triangles), displaying (a) the short-circuit current (J_{sc}), (b) the open-circuit voltage (V_{oc}), (c) the fill factor (FF) and (d) the power conversion efficiency (PCE). The significance of comparing devices produced on the same day is due to the variance in humidity between days. All current density-voltage measurements were performed at a scan rate of 150 mV/s.

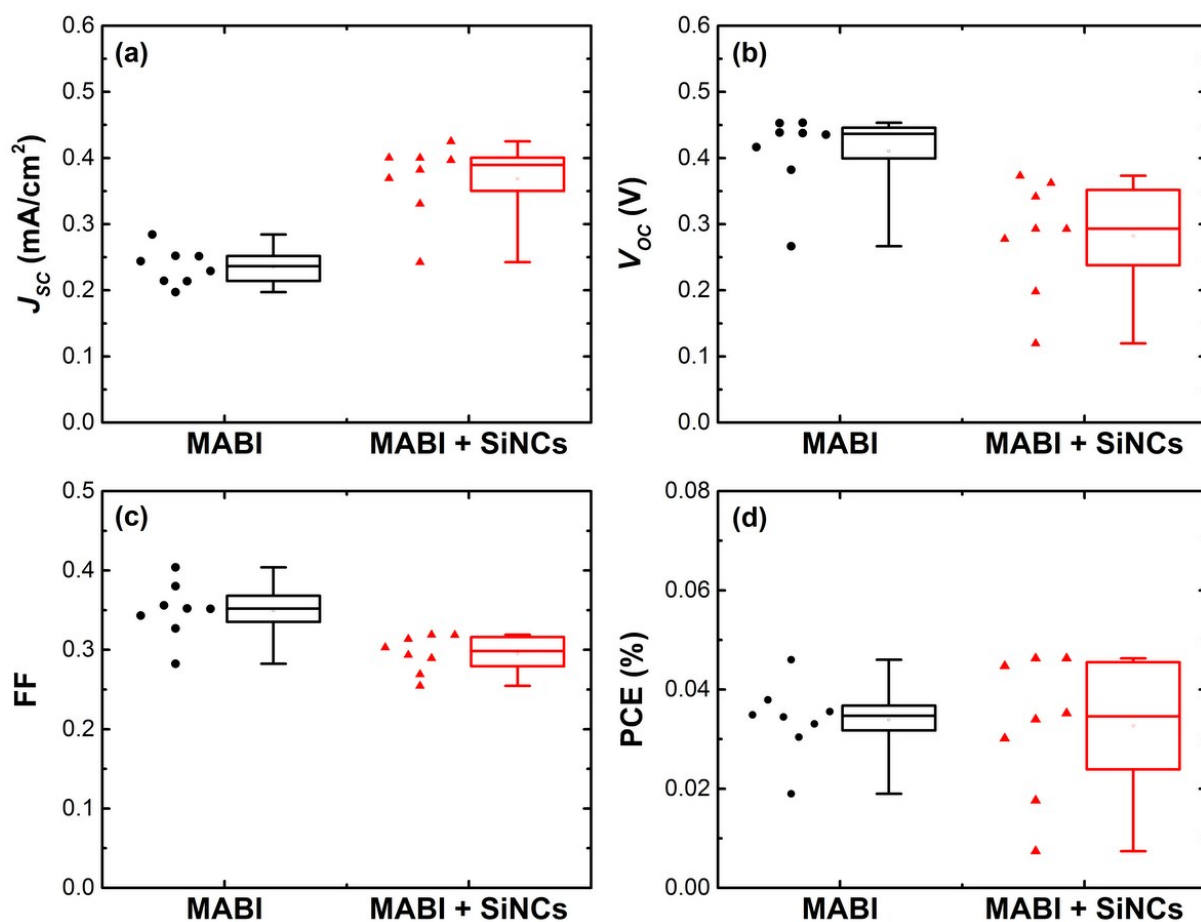


Fig. S6. Performance statistics for the devices shown in Fig. S5 after 16 days of storage in the dark in open air conditions for 8 MABI devices (black circles) and 8 MABI devices with incorporated silicon nanocrystals (red triangles) displaying (a) the short-circuit current (J_{sc}), (b) the open-circuit voltage (V_{oc}), (c) the fill factor (FF) and (d) the power conversion efficiency (PCE). All current density-voltage measurements were performed at a scan rate of 150 mV/s.

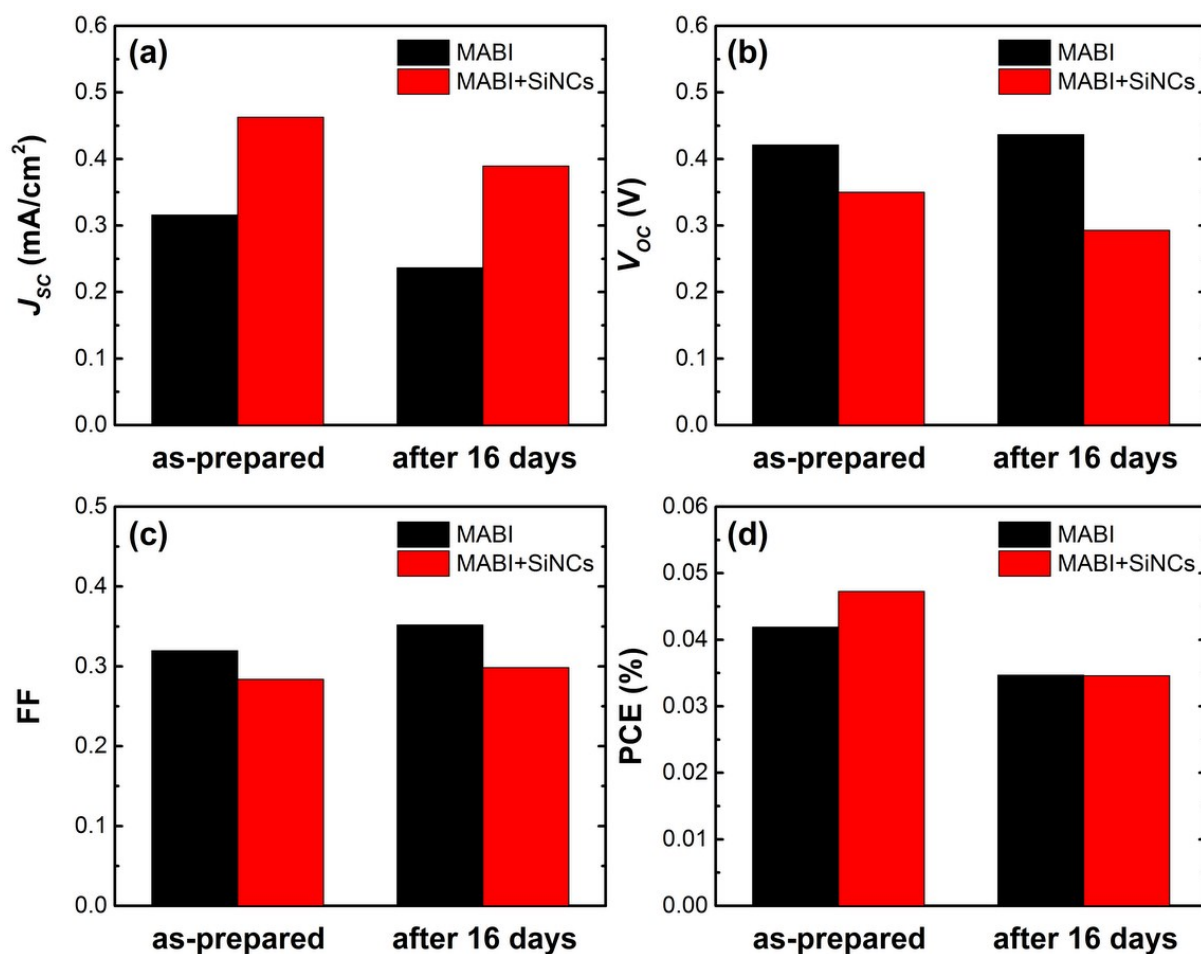


Fig. S7. Comparison of the median performance of MABI devices without SiNCs (black) and with SiNCs (red) displaying (a) the short-circuit current (J_{sc}), (b) the open-circuit voltage (V_{oc}), (c) the fill factor (FF) and (d) the power conversion efficiency (PCE) for devices measured immediately after fabrication as shown Fig. S5 and then after 16 days stored in open air conditions in the dark as shown in Fig. S6. All devices shown were fabricated on the same day due to ensure that the humidity conditions were the same for all devices. All current density-voltage measurements were performed at a scan rate of 150 mV/s.

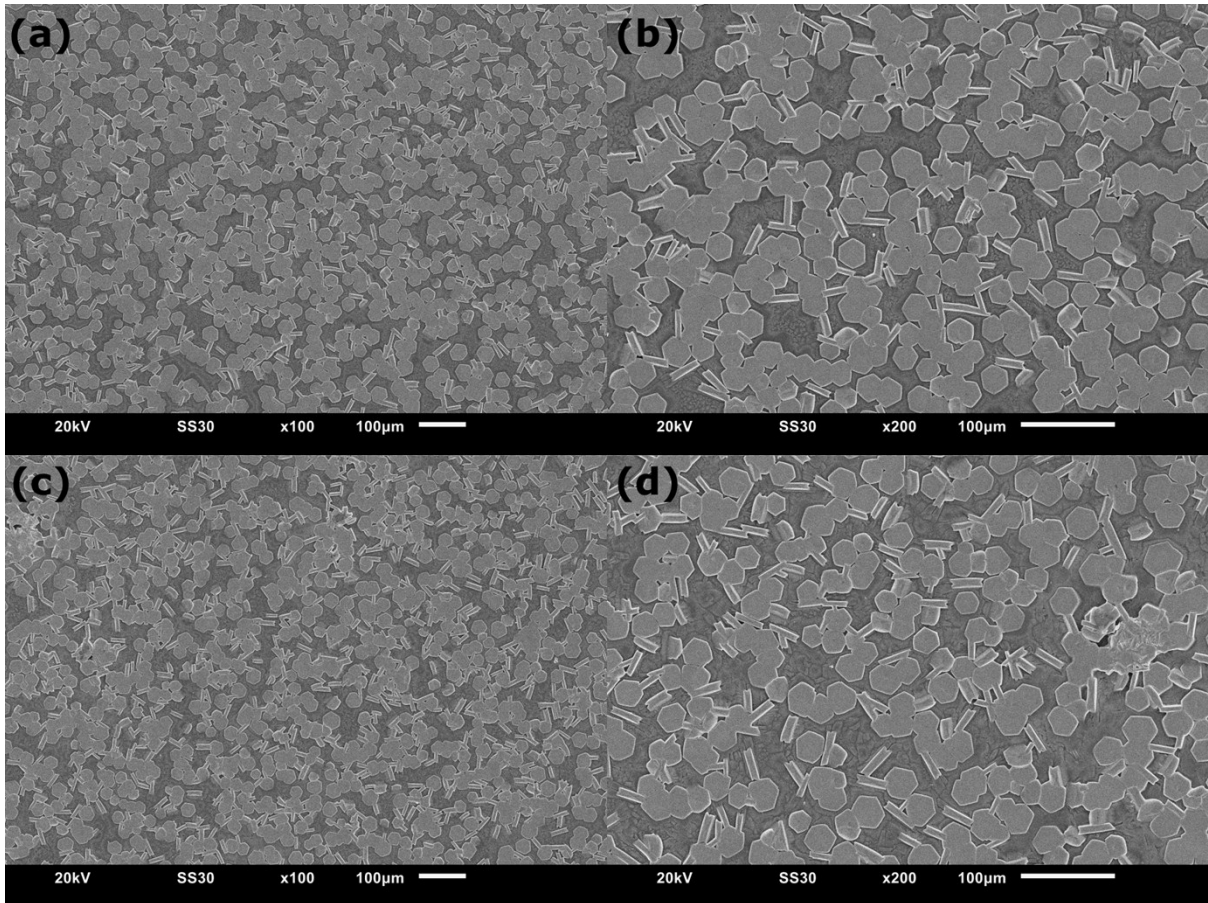


Fig. S8. Scanning electron microscope images of (a,b) MABI layer and (c,d) MABI layer incorporated with SiNCs. The layers were deposited onto glass substrates which were coated with compact TiO_2 and mesoporous TiO_2 to replicate the solar cell structure. The final structure was glass/compact- TiO_2 /mesoporous- TiO_2 /MABI for (a,b) and glass/compact- TiO_2 /mesoporous- TiO_2 /MABI + SiNCs for (c,d). The hexagonal structures are MABI crystals.

References

- (1) Kumar, G. R.; Savariraj, A. D.; Karthick, S. N.; Selvam, S.; Balamuralitharan, B.; Kim, H.-J.; Viswanathan, K. K.; Vijaykumar, M.; Prabakar, K. Phase Transition Kinetics and Surface Binding States of Methylammonium Lead Iodide Perovskite. *Phys. Chem. Chem. Phys. Phys. Chem. Chem. Phys.* **2016**, *18* (18), 7284–7292.
- (2) Hoye, R. L. Z.; Brandt, R. E.; Osherov, A.; Stevanovic, V.; Stranks, S. D.; Wilson, M. W. B.; Kim, H.; Akey, A. J.; Perkins, J. D.; Kurchin, R. C.; Poindexter, J. R.; Wang, E. N.; Bawendi, M. G.; Bulovic, V.; Buonassisi, T. Methylammonium Bismuth Iodide as a Lead-Free, Stable Hybrid Organic-Inorganic Solar Absorber. *Chem. - A Eur. J.* **2016**, *22* (8), 2605–2610.
- (3) Ni, C.; Hedley, G.; Payne, J.; Svrcek, V.; McDonald, C.; Jagadamma, L. K.; Edwards, P.; Martin, R.; Jain, G.; Carolan, D.; Mariotti, D.; Maguire, P.; Samuel, I.; Irvine, J. Charge Carrier Localised in Zero-Dimensional $(\text{CH}_3\text{NH}_3)_3\text{Bi}_2\text{I}_9$ Clusters. *Nat. Commun.* **2017**, *8* (1), 170.